

## **PHYSICAL QUANTITY SENSORS OF EXTENDED FUNCTIONALITY BASED ON SILICON WHISKERS**

**Anatoliy Druzhynin<sup>1,2</sup>, Oleksiy Kutrakov<sup>1</sup>, Yurii Khoverko<sup>1,2</sup>, Serhii Yatsukhnenko<sup>1</sup>**

<sup>1</sup>Lviv Polytechnic National University, Lviv, Ukraine, <sup>2</sup>International Laboratory  
of High Magnetic Fields and Low Temperatures, Wroclaw, Poland  
*druzh@polynet.lviv.ua*

© Druzhynin A., Kutrakov O., Khoverko Y., Yatsukhnenko S., 2016

**Abstract.** The constructive and technological features of creating a sensitive element of physical quantity sensors of extended functionality based on p-type boron-doped silicon whiskers grown by a chemical vapour deposition (CVD) are considered. In the paper we investigate the effect of the Si whisker resistivity on the temperature of an output signal. The distribution of a temperature field is simulated to calculate stationary and dynamic cases in varying both the geometry of contacts placement and the values of thermal conductivity of insulating material and environment. An analysis of computer simulation of the distribution of mechanical stress and deformation in the elements of a pressure sensor, including thermal stress and deformation is conducted to take into account the effect of thermal stresses on the measurement accuracy. The operating temperature range of a sensor (213–423 K) and possible application areas have been defined. A digitizing circuit diagram based on microcontrollers is offered for further signal processing.

**Key words:** microcrystals, multifunctional temperature sensor, pressure sensor, whiskers.

### **1. Introduction**

The need for pressure sensors operating in a wide temperature range is constantly increasing. In particular, there is a strong demand for sensors to control pressure, for example, in internal combustion engines [1–2]. Low temperature sensors are also used in cryogenic equipment [3]. As for now, there is a narrow range of multifunctional sensors that can measure various physical quantities [4]. Such devices are mainly realized by multiple combining of existing sensors in one appliance with a set of microcontrollers for computing incoming data processing. Using one sensitive element as a sensor for measuring several parameters is economically profitable, reduces the size of a measuring device, and improves reliability by simplifying the circuit. On the other hand, it is necessary to evaluate the effect of non-uniform and non-stationary temperature fields on a sensor output signal for measuring one parameter, for example, the effect of non-stationary temperature on the capability

of the sensor to convert mechanical quantities to electrical signals [5].

The important component of the system operating in conditions of sudden temperature changes is thermostatic equipment that requires precise and immediate response to the change in the environment under measurement. The possible use of thermostatic equipment in the environments of high pressure (compressed gas equipment, liquid reservoir and containers, etc.) is the complicated case of sensor application. Industrial mechanical sensors that are present on the domestic market [6] are efficient in a wide temperature range (from 173 K to 453 K), but for such sensors to be used in a wider range, it is necessary to design a complex of sensor systems intended for extending the temperature interval.

Our research has shown that the obtained silicon whiskers have many interesting features, which can be used for creating different sensors of mechanical or thermal quantities [7–8]. The high piezo sensitivity has been found in p-type boron-doped silicon whiskers [9], which may have an impact on the production of miniaturized sensitive piezoresistors based on these tiny crystals [10].

The important feature of crystal whiskers is their strength, which is close to theoretical [8, 10]. This feature allows the sensor to be used in vibrating and unstable environments.

The main purpose of this work is design of silicon whisker-based sensors of extended functionality and a wide temperature range.

### **2. Experimental modelling**

The p-type silicon whiskers with boron impurity grown by chemical vapour deposition in a closed bromide system were chosen as sensitive elements of sensors [10]. The designed special technology for creating ohmic contacts by the method of impulse welding of a platinum microwire with a crystal facet offers the prospect of applying these sensors in adverse operating conditions, particularly at elevated temperatures.

The studies described in [10] showed that for the temperature range of mechanical sensors to be extended towards higher temperatures, it is important to design new methods of fastening the sensitive elements. That is why it was proposed to use solder-glass or glass cement which do not lose their elastic properties up to the temperature of melting. The agreed junction of the Si-solder-glass-elastic element is formed when the coefficients of thermal expansion of all the components are similar. For these reasons, we tested a kovar alloy 29NK with the coefficient of thermal expansion  $(4.6\text{--}5.5)\cdot10^{-6}\text{ K}^{-1}$  and elastic modulus  $E=0.148\text{ GPa}$  as the material for elastic elements. An oxide film, which interacts well with the glass, is formed on the surface while heating the kovar alloy. Kovar alloy in comparison with ceramics and glass ceramics has more technological advantages and is easily processed mechanically. To fix the Si whiskers on the elastic elements there is chosen a solder-glass S51-1 with the coefficient of thermal expansion (CTE)  $4.9\cdot10^{-6}\text{ K}^{-1}$ , which is close to the coefficient of thermal expansion of silicon  $(2.5\text{--}4.2)\cdot10^{-6}\text{ K}^{-1}$  in a temperature range of 293 K – 823 K. The melting temperature of solder-glass S51-1 is 843 K.

Fixing silicon whiskers on elastic elements causes a change in the initial resistance of these crystals and leads to the temperature dependence of the resistance due to the occurrence of thermal deformation  $\epsilon_0$ , which has an effect on the microcrystal. This deformation is determined by CTE of the elastic element material (kovar)  $\alpha_{co}$  and silicon  $\alpha_{si}$ , operating temperature  $T$ , and the temperature of solder-glass crystallization  $T_o$ .

$$\epsilon_0(T) = \int_{T_o}^T \alpha_{co}(t) dt - \int_{T_o}^T \alpha_{si}(T) dt \quad (1)$$

The calculation of the temperature dependence  $\epsilon_0$  which affects Si crystals (fixed on the kovar 29NK) has shown  $\epsilon_0=-3\cdot10^{-3}$  of relative units (RUs) at room temperatures;  $\epsilon_0=-1.5\cdot10^{-3}$  of RUs at  $T = 573\text{--}623\text{ K}$ , which is well consistent with experimental results [3, 11]. More detailed computer simulations of the distribution of mechanical stress and deformation in the elements of a pressure sensor, including thermal stress and deformation, are conducted by the finite element method using the program ANSYS. The result of the modelling is presented in Fig. 1 as a graphical representation of the distribution of mechanical stresses in the structural elements of the sensor.

It is necessary for these results to be analysed for the purpose of taking into account the influence of thermal stress on the measurement accuracy of a mechanical sensor and the possibility of extracting information on the temperature of a measured environment for multifunctional sensors.

The influence of Si whisker resistivity on the temperature dependence of an output signal of half-bridge

consisting of two sensitive elements based on the Si whisker is studied. The value of the temperature coefficient of resistance (TCR) for the Si whiskers of p-type conductivity in the temperature ranged between 293 K and 623 K is  $+0.17$ ,  $+0.18$  and  $+0.23\% \cdot \text{K}^{-1}$ , for the resistivity  $0.005$ ,  $0.016$  and  $0.023\text{ Ohm}\cdot\text{cm}$ , respectively; Having been fixed on kovar alloy, the TCR of the same microcrystals were  $+0.19$ ,  $+0.20$  and  $+0.24\% \cdot \text{K}^{-1}$ , respectively.

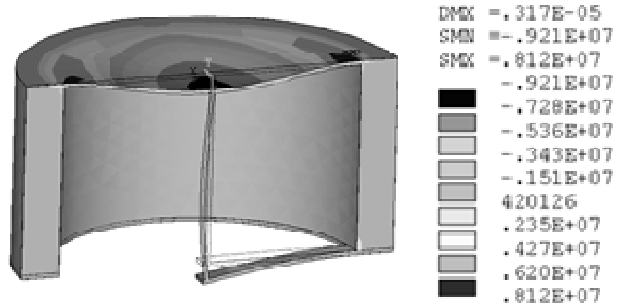


Fig. 1. Distribution of mechanical stresses in the main elements of high-temperature pressure sensor with versatile piezo module.

The mechanism of conductivity is determined by energy levels of boron impurities and hopping conductivity within the impurity band (at low temperatures). Depending on  $\rho$ , the crystals can be divided into three groups: with low-resistivity  $\rho < 0.03\text{ Ohm}\cdot\text{cm}$ , intermediate resistivity  $0.03 < \rho < 0.6\text{ Ohm}\cdot\text{cm}$  and high resistivity  $\rho > 0.6$ . In terms of semiconductor thermometry, the middle group crystals can be used to manufacture wide-band thermometers, in particular cryogenic ones. Their TCR is high enough ( $\alpha_T = e/kT^2$  and is up to  $7\% \cdot \text{K}^{-1}$ ). In this case the activation energy in the equation  $R_0 \exp(e/kT)$  is up to  $e = 0.52\text{ eV}$ , and it is close to the activation energy of gold as one of the dopants for the growth initiator. The ratio  $\rho_{4.2}/\rho_{300}$  for  $\rho = 0.025\text{ Ohm}\cdot\text{cm}$  is  $\sim 1900$ . The crystals with  $\rho = 0.6\text{ Ohm}\cdot\text{cm}$  have both negative and positive values of TCR. The low-resistivity samples have only positive values of TCR  $(4\text{--}6)\cdot10^{-2}\% \cdot \text{K}^{-1}$ . The Si crystals doped with Zn have linear dependences  $R(T)$  with quite high values of TCR ( $\sim 0.5\% \cdot \text{K}^{-1}$ , while for the known Si thermometers, it is  $-0.3\% \cdot \text{K}^{-1}$ ).

### 3. Theoretical modeling

The value of a temperature field in the sensitive element can be found from a common equation of thermal conductivity:

$$r \cdot C \frac{\partial T}{\partial t} - \nabla(k \nabla T) = f, \quad (2)$$

where  $r$  is the density,  $C$  represents the heat capacity,  $k$  denotes the TCR,  $f$  stands for the source of heat.

Boundary conditions, in general case, are a combination of temperature and its gradient on the boundaries of the  $\partial\Omega$  of an object under modelling:

$$-\text{Dirichlet: } hT = r, \quad (3)$$

$$-\text{Neumann: } \mathbf{n} \cdot (\mathbf{k}\nabla T) + qT = g, \quad (4)$$

where  $\mathbf{n}$  is the external normal,  $g, h, q, r$  are the functions defined on  $\partial\Omega$ . Equation (2) is a partial differential equation (PDE) of parabolic type. If there is a stationary case, equation (2) is reduced to elliptic type:

$$-\nabla(k\nabla T) = f. \quad (5)$$

The solution of a PDE using the finite element method consists in the sampling of a differential equation and boundary conditions to obtain a linear system  $\mathbf{K} \cdot \mathbf{T} = \mathbf{F}$ . The  $\mathbf{T}$  vector (which is unknown) contains the values of an approximate solution at the points of grid, the matrix  $\mathbf{K}$  being composed of the coefficients  $k$  and  $h$  ( $h$  is determined by the model purposes). The improvement in accuracy is achieved either by reducing the size of the elements or by increasing the number of elements in the approximations inside the grid cells. Multiply equation (3) by the arbitrary function  $\chi$ , and integrate it over the entire domain  $\Omega$ :

$$-\int_{\Omega} (\nabla(k\nabla T)) c dx = \int_{\Omega} f c dx. \quad (6)$$

Integrating equation (5) by parts and taking into account equation (3), we obtain the following system of equations:

$$\begin{aligned} \int_{\Omega} (k\nabla T) \nabla c dx - \int_{\partial\Omega} n(k\nabla T) c ds &= \int_{\Omega} f c dx \\ \int_{\Omega} (k\nabla T(\nabla c - f c)) dx - \int_{\partial\Omega} (-qT + g) c ds &= 0, \end{aligned} \quad (7)$$

In this solution  $x$  refers to all coordinates  $x, y$ , and  $z$ . The solution  $T$  is obtained from condition (6), which together with the function  $\chi$  belongs to the finite functional space  $V_n$ . Representing the function  $T(x)$  by the system of some test functions, for example

$$T(x) = \sum_{j=1}^{N_p} T_j f_j(x), \quad (8)$$

after the transformations described above, we obtain the following system of equations

$$\begin{aligned} \sum_{j=1}^{N_p} \left( \int_{\Omega} (k \nabla f_j) \nabla f_i dx + \int_{\partial\Omega} q f_j f_i ds \right) T_j &= \\ = \int_{\Omega} f f_i dx + \int_{\partial\Omega} g f_i ds, \end{aligned} \quad (9)$$

where  $i = 1, \dots, N_p$ .

System of equations (9) can be written as the matrix equation  $(\mathbf{K} + \mathbf{Q})\mathbf{T} = \mathbf{F} + \mathbf{G}$ , where  $\mathbf{K}, \mathbf{Q}$  are  $N_p \times N_p$ -matrices, and  $\mathbf{F}$  and  $\mathbf{G}$  denote vectors of  $N_p$ -size:

$$\begin{cases} K_{i,j} = \int_{\Omega} (k \nabla f_j) \nabla f_i dx \\ Q_{i,j} = \int_{\partial\Omega} q f_j f_i ds \\ F_i = \int_{\Omega} f_i dx \\ G_i = \int_{\partial\Omega} g f_i ds \end{cases}. \quad (10)$$

The solution of the system is the vector  $\mathbf{T}$  consisting of the ratios  $T_i$  whose values correspond to the coordinates  $x_i$  of the grid triangle apexes (the model geometry is split by). The computer models were simulated in a specialized software environment Matlab using the package of PDE (Partial differential equations) Toolbox [12].

Fig. 2 shows some results of the calculations for stationary and dynamic cases when varying both the geometry of contacts placement and values of thermal conductivity of insulating material and the environment.

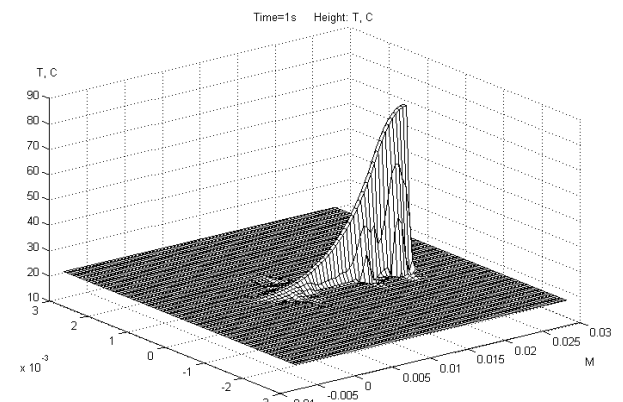


Fig. 2. Temperature field at  $t = 1$  sec.

Furthermore, the distribution was calculated for different time values, and the transition of our system to stationary operations since turned on was evaluated.

The advantage of whisker-based sensors is their low inertia ( $\tau \sim 10^{-2}$  sec), in some cases for the sensors without shell it is  $\sim 10^{-3}$  sec, high stability, workability in high magnetic fields, simple and inexpensive manufacturing techniques.

#### 4. Development of the sensor construction

The experimental research has shown that highly-alloyed Si crystals can be used in creating multifunctional

sensors workable in the extended temperature range. Using certain circuit solutions of a secondary converter, it is possible to obtain several physical quantities from one sensitive element.

An example of a multifunctional sensor is the sensor described in [13], but the functionality of this device is limited. Circuit solutions have a huge potential in extending functional possibilities of the existing sensitive elements of multifunctional sensors.

Methods for the formation of special measuring circuits and processing of measuring information are successful (even from one sensitive element) in distinguishing information on related physical quantities or various parameters of one physical quantity.

In addition, the proposed sensor of pressure (pressure drop) and temperature is able to measure differential pressures and differential temperatures that leads to the extension of its functionality.

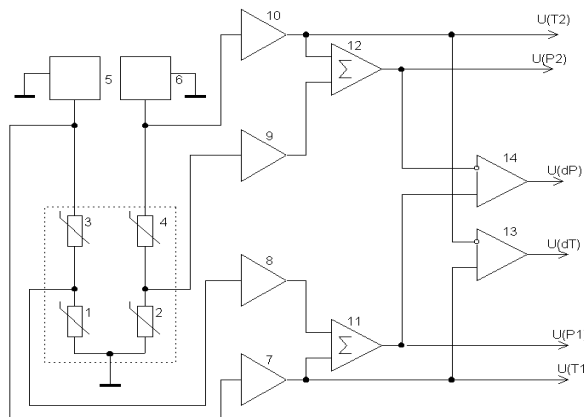


*Fig. 3. Sensor of pressure and temperature.  
(1–4 – strain gauges; 5, 6 – current source; 7–10 – amplifiers;  
11, 12 – adders, 13, 14 – differential amplifiers).*

The sensor of pressure drop and temperature (Fig. 3) works as follows. Strain gauges 1–4 are the Wheatstone Bridge. The pressure  $P_1$  and temperature  $T_1$  of the first environment affect strain gauges 1 and 3 located on the membrane. The pressure  $P_2$  and temperature  $T_2$  of the second environment affect strain gauges 2 and 4 located on the membrane as well.

Besides, strain gauges 1 and 2 are located on the membrane where the pressure leads to their deformation of tension, and strain gauges 3 and 4 are located in those areas where the pressure leads to their deformation of compression. The deformation of tension and compression leads both to increasing the resistances of strain gauges 3 and 4 and decreasing the resistances of strain gauges 1 and 2.

When the differential pressure is applied to the membrane between the upper output of strain gauge 1 and the upper output of strain gauge 2, there will occur a

potential difference which is proportional to the differential pressure, and via amplifiers 8 and 9 is applied to adders 11 and 12 for eliminating the error occurring as a result of variations of the temperature coefficient of strain gauges resistance.

Voltage, which is proportional to the differential pressure, is the output signal of the sensor  $U(dP)$  from amplifier 13. At the output of adder 11 we obtain the voltage  $U(P_1)$  which is proportional to the absolute pressure  $P_1$  of the first environment. Similarly, at the output of adder 12 we obtain the voltage  $U(P_2)$  which is proportional to the absolute pressure  $P_2$  of the second environment.

Since strain gauges 1 and 3 are located on the membrane, which is affected by pressure  $P_1$ , the change in its temperature will lead to the change in the voltage drop between the ground and the upper output of strain gauge 3. This voltage is amplified to the required level by amplifier 7 and fed to the output  $U(T_1)$ . Similarly, at the output  $U(T_2)$  there appears a signal proportional to the temperature of the second environment.

Between the outputs of amplifiers 7 and 10 we obtain a potential difference, which is proportional to the difference of the temperatures between the membranes. This is the voltage which is fed via amplifier 13 to the output of the sensor through the channel of differential temperature measurement  $U(dT)$ .

Fig. 4 shows a design of the developed multifunctional sensor of pressure (pressure drop) and temperature.

Thus, the sensor of pressure and temperature has advanced functionality and allows high-precision measurement of differential pressure, differential temperature, and their absolute values simultaneously.

As is known, a temperature correction of the characteristics typical of silicon-based measuring transducers of mechanical quantities using analogue circuits requires more careful tuning of their parameters and does not provide high accuracy of measurement over the entire operating temperature range of a sensor [14].

A necessary part of the measuring process is digitization of a measured signal, reduction of interference, etc. The deformation of an elastic element (either silicon- or metal-based) is measured using a piezo bridge formed on its surface.

In general, the signal generated by the piezo bridge is noisy-contaminated, has a small amplitude, shift of both zero and maximum value. In addition, the sensitivity and shift of the piezo bridge zero is temperature dependent. Recently, on the global market of microelectronics have appeared specialized instrumental amplifiers and high-speed microcontrollers possessing a great number of advanced features.

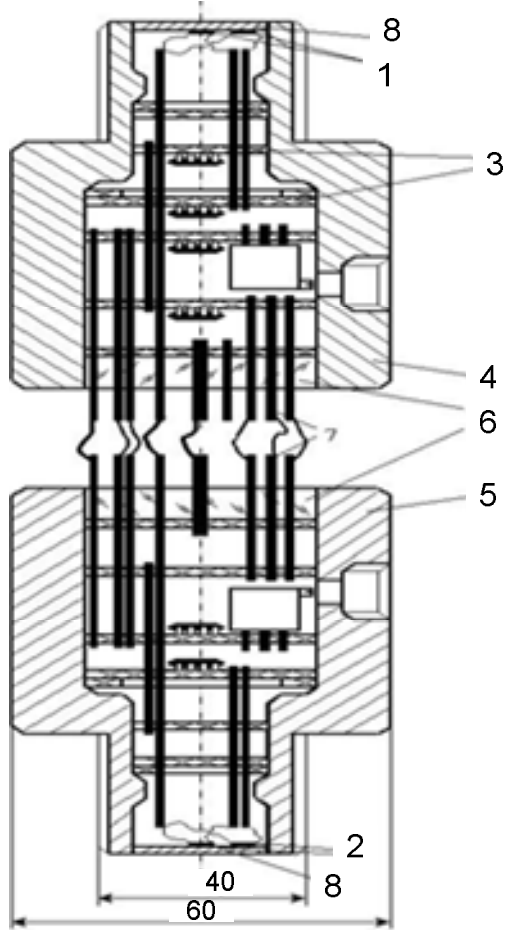


Fig. 4. Design of developed sensor: 1 – the first and third strain gauges; 2 – the second and fourth strain gauges; 3 – microcontrollers; 4, 5 – separated sensor sheaths; 6 – epoxy resin; 7 – outputs of sensor; 8 – membrane.

Selecting components to develop a multifunctional sensor is mainly defined by the requirements of the features and parameters of a sensor under development, as well as its price. Fig. 5 shows a block diagram of the sensor.

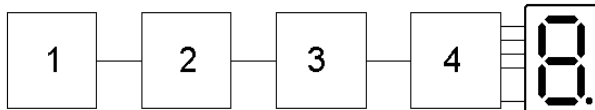


Fig. 5. Block diagram of a sensor:  
1 – primary converter power circuit, 2 – Wheatstone bridge,  
3 – transducer, 4 – signal processing circuit.

The block-diagram presented in Fig. 5 was designed by using modern microcontrollers to improve metrological characteristics of the sensor. The multifunctional sensor developed by us processes signals with the help of the microcontroller Atmega8 manufactured by Atmel [15].

Fig. 6 shows a circuit diagram of the developed intelligent sensor. The primary converter is a

Wheatstone bridge which consists of strain gauges with a high temperature coefficient of resistance that function both as a sensor of deformation and as a sensor of temperature. The strain gauges were made on the basis of silicon whiskers with the resistivity of 0.01–0.02 Ohm·cm, and the piezoresistive coefficient of 100–140.

On being amplified in the region DA1, the proportional to the deformation of strain gauges voltage from the diagonal of the measuring bridge is fed to the input ADC0 of the microcontroller DD1 to convert it to the digital form using an ADC. The capacitor C1 together with the internal resistor RF IMC AD8555 is a low pass filter (LPF) required to satisfy the Nyquist criterion for the ADC. The temperature compensation of errors of a pressure drop sensor, and obtaining information on the environment temperature are implemented by using a signal from the bridge circuit consisting of four strain gauges. The temperature signal is amplified by the scheme DA2 and fed to the second input of the ADC (ADC1). The information is entered into computer by using interface RS232 (transform of levels and galvanic outcome are carried out by using an opto-isolator DA4).

The main functions of the microcontroller DD1 are separating the signals of temperature and pressure, and selecting the useful signals of temperature, pressure and deformation. Besides, the microcontroller DD1 is responsible for the correction of errors dependent on temperature.

The main disadvantage of the sensitive elements based on semiconductor whiskers is their wide variation of parameters. That is why the allocation of a calibration table, which is individual for each transducer, in the flash-memory of a microcontroller provides high-precision conversion. This solution allows us to achieve high accuracy of measurement. The small dimensions of a microcontroller that can operate in the various

The proposed sensor provides accurate measurement of temperature and pressure in the temperature range from 213 K to 423 K with the measurement errors not exceeding 0.01 %. Software-based sensor adjustment environments allow us to embed it directly into the body of the sensor. The circuit diagram is oriented to be used with the sensors of physical quantities based on silicon whiskers but can also be used with any other silicon pressure sensitive elements with a high TCR. makes it easy to automate the process of calibration and use primary converters with a wide variation of parameters.

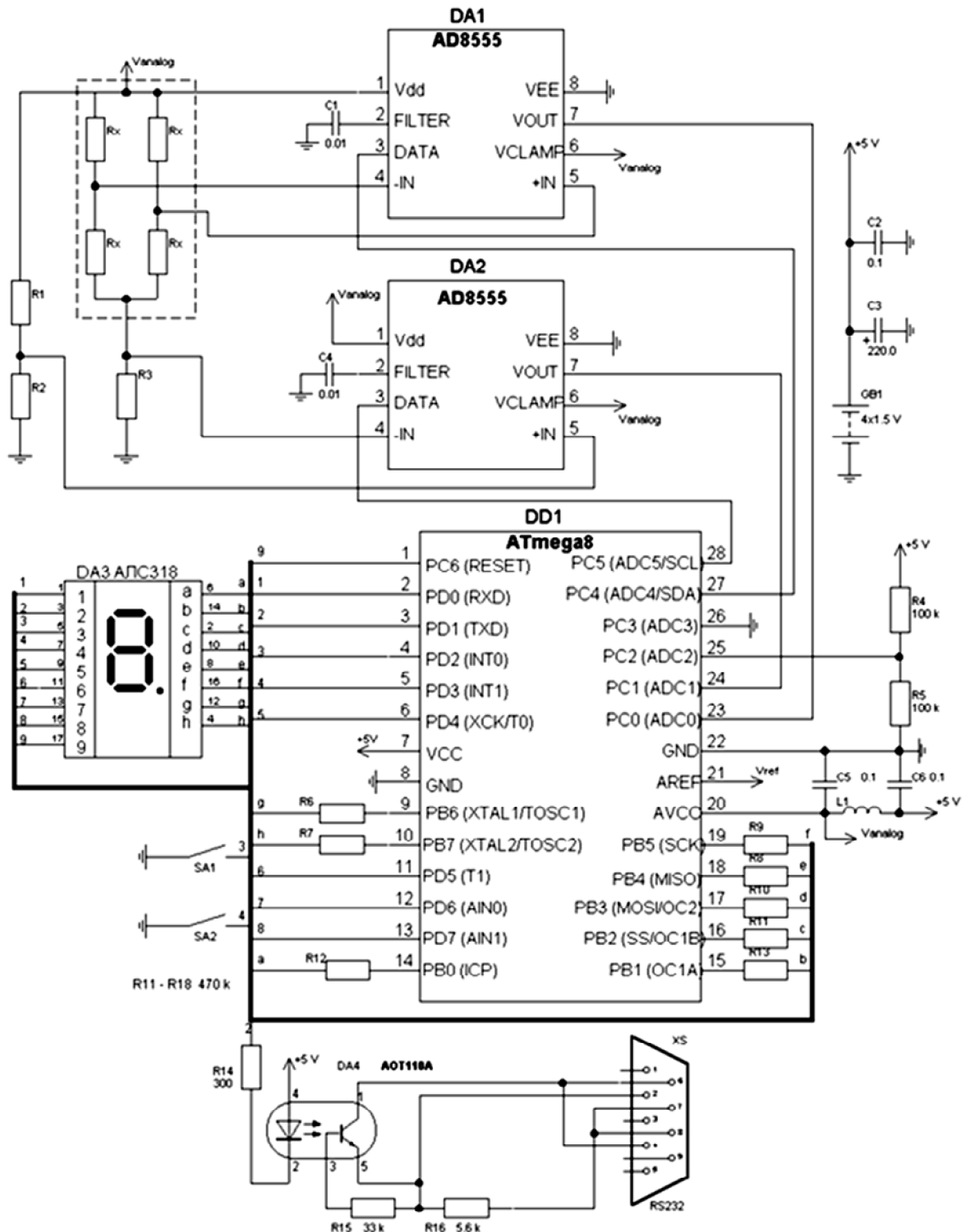


Fig. 6. Circuit diagram of the developed intelligent sensor.

## 5. Conclusion

This research deals with creation of a highly sensitive sensor to use in a wide temperature range. This sensor can simultaneously measure pressure (pressure drop), absolute temperature and temperature differences and can be used to study the distribution of pressure and temperature of different environments in high magnetic fields. The developed digital signal processing circuit

makes it possible to adjust temperature-dependent errors; to differentiate the appropriate signal of temperature, pressure and deformation.

## References

- [1] G. Lammel, S. Armbruster, C. Schelling, H. Benzel, J. Brasas, M. Illing, R. Gampp, V. Senz, F. Schafer, and S. Finkbeiner, "Next generation pressure sensors in surface micromachining technology", in *Proc. 13th International Conference on Solid-State Sensors, Actuators, and Microsystems*; pp. 35–36, Seoul, Korea. 2005.
- [2] Y. C. Sun, Z. Gao, L. Q. Tian, and Y. Zhang, Modelling of the reverse current and its effects on the thermal drift of the offset voltage for piezoresistive pressure sensors. *Sensors and Actuators A*, vol. 116, pp. 125–132, 2004.
- [3] I. Maryamova, A. Druzhinin, and E. Lavitska, Low-temperature semiconductor mechanical sensors. *Sensors and Actuators A*, vol. 85, pp. 153–157, 2000.
- [4] P. Eswaran, et. al., "MEMS Capacitive Pressure Sensors: A Review on Recent Development and Prospective", *International Journal of Engineering and Technology (IJET)*, vol. 5, no. 3, 2013.
- [5] A. Druzhinin, I. Maryamova, E. Lavitska, and Y. Pankov, "Physical aspects of multifunctional sensors based on piezothermomagnetic effects in semiconductors", *Sensors and Actuators A*, vol. 68, pp. 229–233, 1998.
- [6] P. Girak and O. Ostapenko, "The industrial pressure sensors with technology Trafag", *Mir Avtomatizatsyi*, no. 1–2, pp. 52–55, 2016. (Ukrainian)
- [7] M. W. Shao, Y. Y. Shan, N. B. Wong, and S. T. Lee, "Silicon Nanowire sensors for bioanalytical applications: Glucose and hydrogen peroxide detection", *Advanced Functional Materials*, vol. 15, pp. 1478–1482, 2005.
- [8] T. Toriyama, Y. Tanimoto, and S. Sugiyama, "Single crystal silicon nano-wire piezoresistors for mechanical sensors", *Microelectromechanical Systems Journal*, no. 11, pp. 605–611, 2002.
- [9] J. X. Cao, X. G. Gong, and R. Q. Wu, "Giant piezoresistance and its origin in Si(111) whiskers: First-principles calculations", *Physical Review B*, vol. 75, article 233302, 2007.
- [10] A. Druzhinin, O. Kutrakov, and I. Maryamova, "Tensoresistive pressure sensors based on silicon whiskers for a wide range of temperatures", *Bulletin of Lviv Polytechnic National University: Electronics*, no. 708, pp. 64–71, 2011. (Ukrainian)
- [11] M. Tukhan, "Experimental study of characteristics piezoresistive pressure sensors non-stationary processes", *Bulletin of "Ihor Sikorskyi Kyiv Polytechnic Institute" National Technical University of Ukraine: Pryladobuduvannya*, vol. 51, no. 1, pp. 5–11, 2016. (Ukrainian)
- [12] <http://www.mathworks.com>, MATLAB PDE Toolbox.
- [13] "Temperature sensors, type AKS 21", *Danfoss products*, Literature No. DKRCIED.SA0.A2.22, p. 1–4, 2007.
- [14] E. Slyva, "Temperature adjustment of physical values measuring transducers based on MSP430F149 microcontrollers designed by Texas Instruments", [http://www.chipnews.ru/html.cgi/arhiv/01\\_05/stat-3.htm](http://www.chipnews.ru/html.cgi/arhiv/01_05/stat-3.htm)

## ДАВАЧІ ФІЗИЧНИХ ВЕЛИЧИН

### З РОЗШИРЕНИМИ

### ФУНКЦІОНАЛЬНИМИ

### МОЖЛИВОСТЯМИ

### НА ОСНОВІ НІТКОПОДІБНИХ

### МІКРОКРИСТАЛІВ КРЕМНІЮ

Анатолій Дружинін, Олексій Кутраков,  
Юрій Ховерко, Сергій Ящухненко

Розглянуто конструктивно-технологічні особливості створення чутливого елемента давача фізичних величин з розширеними функціональними можливостями на основі ніткоподібних кристалів кремнію *p*-типу провідності з домішкою бору вирощених механізмом пара–рідина–кристал. Проведено дослідження впливу питомого опору НК Si на температурну залежність вихідного сигналу. Отримано результати комп’ютерного моделювання розподілу температурного поля для розрахунку стаціонарного й динамічного випадків у разі варіювання як геометрії розміщення контактів, так і значеннями коефіцієнтів тепlopровідності ізоляльного матеріалу та навколошного середовища. Аналіз комп’ютерного моделювання розподілу механічних напружень і деформацій в елементах давача тиску, зокрема термічних навантажень і деформації проводили для врахування впливу температурних напружень наточність вимірювання давача механічних величин та можливості виділення інформації про температуру вимірюваного середовища для багатофункційних сенсорів. Визначено температурний інтервал роботи давача (213–423 K) та можливі галузі використання. Запропоновано схему оцифрування для подальшого оброблення сигналу.



Anatoliy Druzhinin – D. Sc., professor, State Prize of Ukraine in Science and Technology, Honored Worker of Science and Technology of Ukraine, Head of the Department of Semiconductor Electronics at the Institute of Telecommunications, Radioelectronics and Electronic Engineering, Lviv Polytechnic National University, Ukraine. He is also the winner of

Ukrainian State Prize in Science and Technology (2011). The main scientific activities of prof. Druzhynin include: theoretical and experimental study of strain-induced effects in silicon, germanium and their solid solutions whiskers. Prof. Druzhynin has authored more than 600 scientific papers including more than 40 inventor's certificates and patents. Under his supervision 4 doctors and 11 candidates in technical science have been graduated.



**Oleksiy Kutrakov** – Ph.D., Senior Researcher of the Department of Semiconductor Electronics at the Institute of Telecommunications, Radio-electronics and Electronic Engineering, Lviv Polytechnic National University, Ukraine. The researcher has authored more than 100 scientific papers including 5 patents. The main scientific activities of O. Kutrakov

include theoretical and experimental study of strain-induced effects in silicon, germanium, their solid solutions whiskers and designing sensors of physical quantities based on semiconductors.



**Yuriy Khoverko** – D. Sc, Senior Researcher. Department of Semiconductor Electronics of Lviv Polytechnic National University. Research interests cover physics and technology of semiconductor devices, micro- and nanoelectronic structures and sensor electronics. His research findings have been published in more than 180 scientific papers. He is the co-author of 8 patents of Ukraine.



**Serhii Yatsukhnenko** – postgraduate student of the Department of Semiconductor Electronics at the Institute of Telecommunications, Radio-electronics and Electronic Engineering, Lviv Polytechnic National University, Ukraine.